Nuclear Engineering and Technology 55 (2023) 575–579

Contents lists available at ScienceDirect

Nuclear Engineering and Technology

journal homepage: www.elsevier.com/locate/net

Original Article

Surface morphology and deuterium retention in W and W-HfC alloy exposed to high flux D plasma irradiation

Yongkui Wang [a], Xiaochen Huang [a], Jiafeng Zhou [a], Jun Fang [a], Yan Gao [a], Jinlong Ge [a], Shu Miao [b], Zhuoming Xie [c, *]

[a] School of Material and Chemical Engineering, Bengbu University, Bengbu, 233030, China
[b] Guangdong Provincial Key Laboratory of Advanced Welding Technology, China-Ukraine Institute of Welding, Guangdong Academy of Sciences, Guangzhou, 510650, China
[c] Key Laboratory of Materials Physics, Institute of Solid State Physics, Chinese Academy of Sciences, Hefei, 230031, China

ARTICLE INFO

Article history:
Received 21 June 2022
Received in revised form
4 October 2022
Accepted 11 October 2022
Available online 14 October 2022

Keywords:
Tungsten
W-HfC alloy
D retention
Hardening

ABSTRACT

In this work, pure W and W-0.5wt%HfC alloy (WHC05) were fabricated by sintering and hot-rolling following the same processing route. After exposing to a high flux deuterium plasma irradiation with the D^+ flux to three fluences of 6.00×10^{24}, 2.70×10^{25} and 7.02×10^{25} D/m^2, the evolution of surface morphology, deuterium retention and hardening behaviors in pure W and WHC05 has been studied. The SEM results show the formation of D blisters on the irradiated area, and with the increase of D implantation, the size of these blisters increases from 200 ~ 500 nm (2.70×10^{25} D/m^2) to 1 ~ 2 μm (7.02×10^{25} D/m^2) in WHC05 and from 1 ~ 2 μm (2.70×10^{25} D/m^2) to > 3 μm (7.02×10^{25} D/m^2) in pure W, respectively. A higher D retention and obvious hardening are observed in pure W than that of the WHC05 alloy, indicating an improve radiation resistance in WHC05 compared to pure W.

1. Introduction

Controlled thermonuclear fusion energy is currently recognized as one of the important ways to finally solve energy and environmental problems. Magnetically confined tokamak is a most likely method achieving the controlled thermonuclear fusion. The extremely harsh service environment in the magnetic confinement fusion reactor places extremely high demands on advanced materials. Especially for plasma facing materials (PFMs), it not only has to withstand high-fluence 14 MeV fusion neutron radiation, but also suffers from hydrogen isotope and helium plasma bombardment with a flux of 10^{22} - 10^{24} m^{-2}s^{-1} and an energy of < 500 eV [1,2]. Strong hydrogen plasma will interact with the reactor PFMs and stay in it, causing hydrogen embrittlement, blistering, and swelling, leading to the failure of PFMs. In particular, tritium is expensive and radioactive, and its retention in PFMs would cause fuel loss [3]. Therefore, how to increase the resistance to hydrogen irradiation and reduce the retention of hydrogen isotope are key issues that need to be solved urgently for PFMs in future fusion reactors.

Tungsten (W) and its alloys have many excellent properties such as high melting point, high thermal conductivity, low tritium retention, low sputtering yield, and high self-sputtering threshold [4–6]. They have been regarded as the most promising PFMs to be used in tokamak fusion reactors [7]. However, it has been indicated that the low tritium retention characteristic of W are gradually lost after intense irradiation. For example, after irradiation by heavy ion, the hydrogen retention in the irradiated W samples are significantly increased by 2–3 orders of magnitude [8,9]. Actually, the irradiation environment in fusion device is more rigorous, and it can be predicted that the retention of hydrogen isotopes will increase significantly within the operation, which seriously threatens the safe and stable operation of fusion reactors [10]. Therefore, it is important to improve the radiation resistance of W materials, and thus to reduce the retention of hydrogen isotopes.

It has been indicated that the radiation resistance and hydrogen retention behavior of W materials are closely related to their microstructures [11–13]. The introduction of nanosize second phase particles to W matrix can improve radiation resistance and reduce the hydrogen retention. For instance, fine-grained W-(0-1.5)%TiC has better resistance to high-energy neutron irradiation and to high-flux hydrogen plasma bombardment than that of pure W [11]. Compared with pure W materials, W-3.3wt%TaC alloy exhibits a

* Corresponding author.
E-mail address: zmxie@issp.ac.cn (Z. Xie).

https://doi.org/10.1016/j.net.2022.10.011

relatively lower hydrogen retention after hydrogen plasma bombardments [12]. These improved performances are indicated from the refined micro-structures including fine grains and the high-density of nanophase interface boundaries, which could effectively absorb and disperse irradiation defects, thus reduce the retention of hydrogen by coarse irradiation defects, and inhibit the generation of hydrogen to form voids and bubbles [13].

In our recent work, it has been indicated that a small amount of nano HfC addition to the W matrix not only improve the low temperature ductility of the WHC05 alloy, but also increase its high temperature creep strength [14]. For W materials exposed to low-energy, high flux hydrogen plasmas, local plastic deformation caused by hydrogen super-saturation within the near-surface layer is suggested as a mechanism for formation of intergranular and intragranular cracks [15–18]. Thus, it is possible to suppose that the optimization of microstructure and mechanical properties in our WHC05 can improve the irradiation resistance and reduce the hydrogen retention. In this work, we bombard the pure W and WHC05 to high flux deuterium plasma irradiation to perform a comparative study on the evolution of surface morphology and D retention in these two W materials. Systematic investigations including SEM characterization, thermal desorption spectroscopy (TDS) analysis and nano-indenter tests were conducted.

2. Experimental detail

2.1. Materials preparation

The bulk materials of pure W and W-0.5%wt HfC alloys (designated as WHC05) were fabricated through an identical route of powder metallurgy including sintering and rolling processes which was detailed in our previous work [14]. In this work, the samples were annealed at 1273 K for 1 h in a high vacuum chamber with a vacuum condition of 1×10^{-5} Pa for stress relief as the standard step before storing or grinding and polishing. Specimens with the size of $10 \times 10 \times 1.5$ mm^3 were cut from the stress-relieved WHC05 plate. Then these specimens were mechanically polished, cleaned and electrochemically polished in an aqueous 1.5% NaOH solution at a constant voltage of 11 V to obtain a stress-free surface.

2.2. D plasma irradiation

D plasma exposure experiments were carried out in a linear plasma device of Simulator for Tokamak Edge Plasma (STEP) at Beihang University. Based on the previous results of deuterium irradiation on tungsten materials, in terms of the bubble formation thresholds (ion incident energy and irradiation fluence) [19], we set the irradiation conditions with a constant D^+ flux of 5.0×10^{21} D/m^{2}s by applying Bohm criterion, an incident energy of ~ 90 eV by negatively biasing the sample, and three fluences of 6.00×10^{24} D/m^2, 2.70×10^{25} D/m^2 and 7.02×10^{25} D/m^2, as listed in Table 1. During the deuterium plasma exposure, the surface temperature of the target sample was monitored by a thermocouple press at the rear of the samples, staying around 453 ~ 503 K. The specimens of pure W and WHC05 were exposure to the same deuterium irradiation conditions.

Table 1
List of conditions for ion irradiation. Noting that the temperature variance of ±50 K came from a short time (tens to hundreds of seconds) fluctuation of D^+ flux.

Flux (D^+/m^{2}s)	Time (s)	Fluence (D^+/m^2)	Bias (eV)	Temperature (K)
5.00E+21	1200	6.00E+24	90	453 ± 50
	5400	2.70E+25	90	
	14400	7.02E+25	90	

2.3. Microstructural analysis, TDS and nanoindentation tests

The surface modification was investigated using a field emission scanning electron microscopy (FESEM, SU8020 Hitachi, Japan). Deuterium (D_2) release characteristics were measured by thermal desorption spectroscopy (TDS) with a quadruple mass spectrometer (QMS). Specimens were linearly heated up to 1273 K at a constant heating rate of 0.5 K/s. Nanoindentation (Nano Indenter G200, Agilent, USA) tests were conducted at room temperature to investigate the irradiation hardening induced by deuterium irradiation. The nanoindentation test was carried out using a continuous stiffness mode through a depth-controlled testing method with a maximum testing depth of 2000 nm after pre-calibration on the standard silico. The indenter is a dedicated Berkovich diamond indenter with a guaranteed radius of curvature of 20 nm, and during tests the displacement resolution is set as 0.05 nm.

3. Results and discussion

3.1. Microstructural analysis

Fig. 1 shows a contrast of the D plasma bombardment area with unirradiated peninsula on the surface of pure W and WHC05 specimens after D plasma exposure to a fluence of 6.00×10^{24} D/m^2. There is a clear boundary between the irradiated and unirradiated areas, and the former is covered by vast blisters. The blisters on the irradiated area of pure W are larger in the size but fewer in the number density compared to the case of WHC05. This result forebodes the large amount of hydrogen isotope retained in pure W, and the easy merge of small blisters to form large ones.

Fig. 2 presents the surface morphology after D plasma exposure with fluences of 2.70×10^{25} D/m^2 and 7.02×10^{25} D/m^2. When the irradiated fluence is 2.70×10^{25} D/m^2, the irradiated surface of the WHC05 is mainly composed of 200 ~ 500 nm blisters, while the rolled pure W is covered by 1 ~ 2 μm coarse blisters, as shown in Fig. 2a and b, respectively. Further increasing the irradiation fluence to 7.02×10^{25} D/m^2, the size of blisters on the WHC05 increased to 1 ~ 2 μm (Fig. 2c), whereas most blisters on the pure W further increased to 2 ~ 3 μm in size as shown in Fig. 2d. From the morphology result, it could be concluded that the size of the blisters increases with the increases of D fluences, and the mergers and acquisitions of small blisters could generate large ones. Compared to the pure W, WHC05 exhibits higher resistance to the coarsening of blisters. As a result, the irradiated area of pure W has large and few blisters, while the WHC05 has smaller but dense blisters. It has been indicated that the WHC05 has fine sub-grains (~1 μm) and well dispersed nano-scale HfC particles (average size ~ 51 nm) [18]. These refined sub-grains and nano HfC particles offer abundant boundaries to absorb and disperse these implanted D^+ ions, and thus reduce the D generation. A similar result of high-dense and fine-sized D blisters has been reported in the W–Y_2O_3 composite which also has refined grains and abundant Y_2O_3/W phase boundaries [20].

3.2. TDS test

After SEM characterization, the hydrogen retention in the specimen is then measured by thermal desorption spectroscopy (TDS), and the results are presented in Fig. 3. After the D irradiation to a relatively high fluence of 7.02×10^{25} D/m^2, the D retention in pure W is much higher than that of WHC05. The temperature dependent D desorption peaks appear roughly the same positions for pure W and WHC05 specimens. From the previous work [21], we know that the ultra-fine sub-grains and uniformly dispersed nano particles provide sufficient boundaries, which works as fast

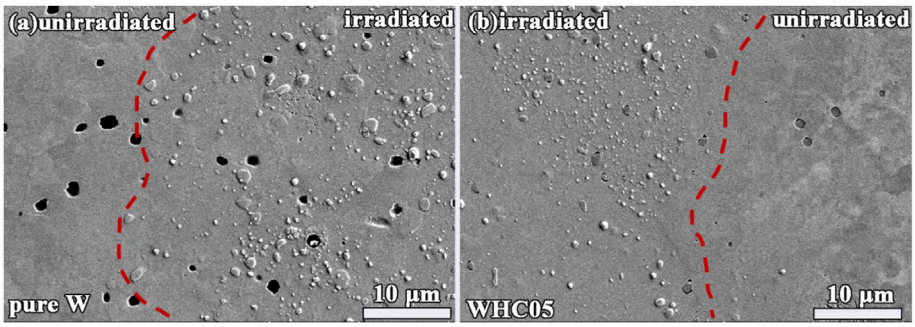

Fig. 1. SEM images showing the surface of (a) pure W and (b) WHC05 specimens after D plasma irradiation to a fluence of 6.00 × 10^{24} D/m^2.

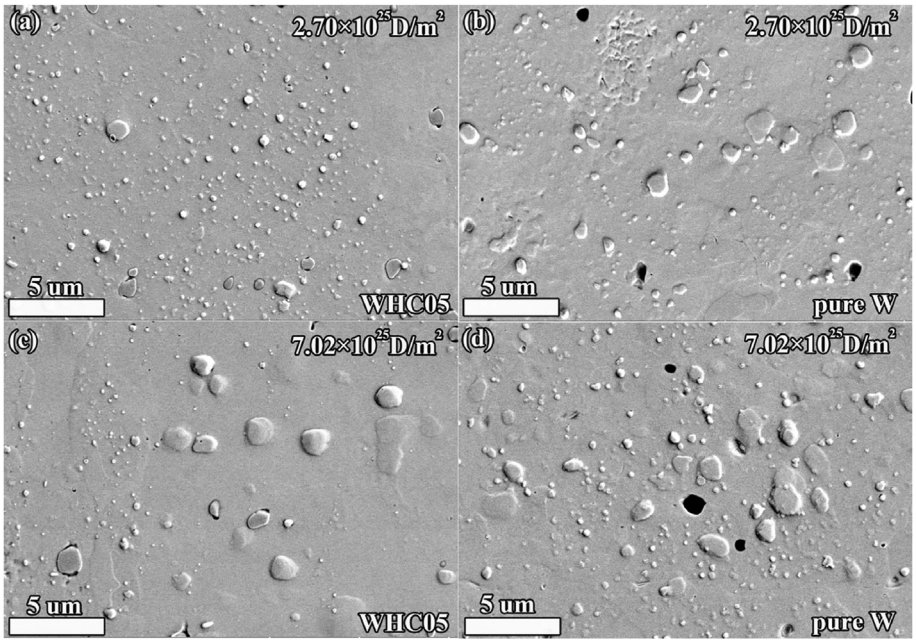

Fig. 2. SEM images showing the surface of pure W and WHC05 specimens after D plasma irradiation to various fluences of 2.70 × 10^{25} D/m^2: (a) WHC05, (b) pure W, and 7.02 × 10^{25} D/m^2: (c) WHC05, (d) pure W.

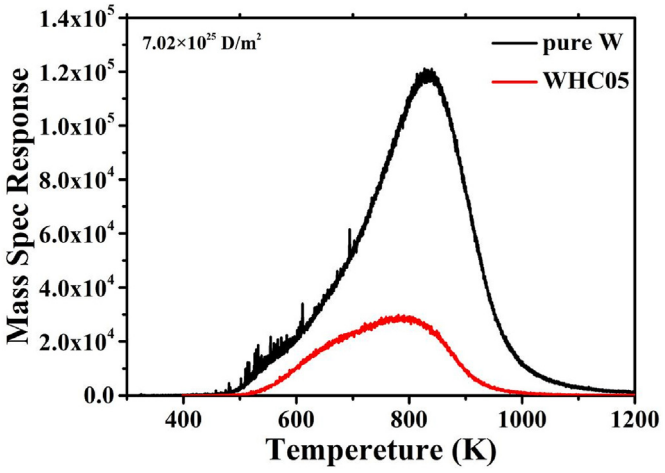

Fig. 3. TDS spectrums of pure W and WHC05 specimens after D irradiation to a fluence of 7.02 × 10^{25} D/m^2.

channels for hydrogen isotope diffusion. During the 453 ~ 503 K D plasma irradiation, most D ions may release from the WHC05 through these fast channels, resulting in a lower amount of D retention in the material. The result indicates that the optimization of microstructure through addition of nano HfC is beneficial to improve the resistance to D radiation.

Intuitively, the TDS profiles display a weak peak and a relatively strong peak in the pure W specimen, located at about 560 K, and 830 K, respectively, as shown in Fig. 3. In addition, some sudden spikes were observed in a wide temperature range of 500 ~ 700 K in the pure W specimens. These spikes come from the sudden release of deuterium gas from the bursting of some coarse bubbles during the heating process [22,23]. It's known that the desorption peak at ~ 560 K is related to D trapping at intrinsic defects which include dislocations, grain boundaries and/or mono-vacancies and D-plasma-induced point defects [24,25]. And the peak at ~ 830 K was considered from the chemisorption of deuterium gas in large voids [26]. The relatively strong D desorption peak at ~ 830 K, together with the obvious spikes, suggests that deuterium exists mainly in molecular form and stays at coarse bubbles and voids in pure W [22,27,28].

The WHC05 has similar high temperature desorption peaks to

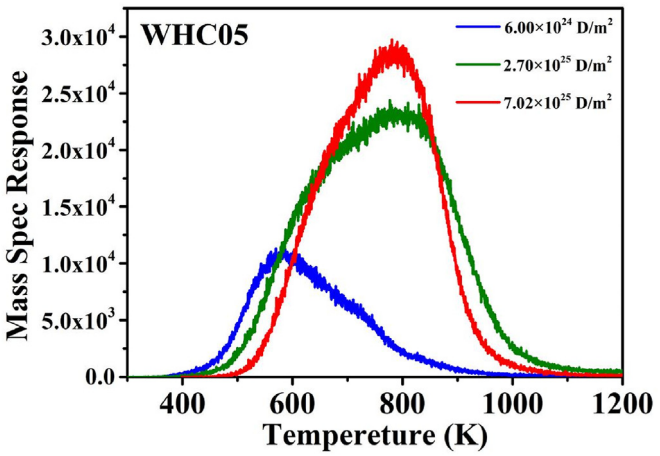

Fig. 4. TDS spectrum of WHC05 specimens after D irradiation to various fluences.

the pure W after D irradiation to a fluence of 7.02 × 10^{25} D/m^2 as shown in Fig. 3. To further indicate the retention of D in WHC05 with the increase of D^+ ion implantation, three TDS profiles of the irradiated WHC05 after exposure to 6.00 × 10^{24} D/m^2, 2.70 × 10^{25} D/m^2 and 7.02 × 10^{25} D/m^2 D^+ irradiation are presented in Fig. 4. In the case of 6.00 × 10^{24} D/m^2 fluence, the desorption profiles of WHC05 show a weak and broad peak which contians two main humping signals at about 580 K and 700 K, as shown in Fig. 4. The peak at ~ 580 K was suggested to be related to D trapping at intrinsic defects [24,25]. The peak at ~ 700 K was considered to be the D trapped at plasma-induced blisters [29]. With increasing the D fluence up to 2.70 × 10^{25} D/m^2, the dominant desorption peak appears at ~ 800 K, which indicate the formation of large aerated voids in the matrix of WHC05 specimen [26].

3.3. Nanoindentation hardness test

Fig. 5a and b shows the nanoindentation hardness as a function of the indentation depth for unirradiated and irradiated specimens. The data in the depth less than 10 nm was sifted out due to the uncertainty from indenter tip complexity. Compared to the unirradiated specimens, the irradiated ones show an evident hardening. This hardening behavior is observed for both the pure W and WHC05 specimens. For the pure W, the hardening can be observed from the surface up to a depth of 2000 nm, indicating that the irradiation defects such as dislocation loops and atom clusters may be distributed throughout the depth of ~ 2000 nm. It has been indicated that the implanted D in tungsten materials is mainly retained near the surface layer, and the D concentration decreases with the increase of depth [30]. A result of radio frequency-glow discharge optical emission spectroscopy analysis presented that the implanted D was detected under the sample surface in a depth range of 0.1 ~ 0.46 μm [22], confirming the possible existence of irradiation defects along the depth range of hundreds of nanometers or even microns. However, the WHC05 has no obvious radiation strengthening below the depth of 1500 nm as shown in Fig. 5b, as compared to the pure W. This may come from the effective dispersion of irradiation defects in WHC05, thus reducing their penetration along the depth.

The deviation of hardening becomes unconspicuous with the increase of the D fluence from 6.00 × 10^{24} to 7.02 × 10^{25} D/m^2 in pure W. For instance, the hardness of the unirradiated pure W is ~ 6.5 GPa. After D irradiation to various fluences, almost the same hardness value of ~ 7.9 GPa is observed in irradiated pure W specimens, resulting in ~ 1.4 GPa hardening value and a corresponding hardening rate of 21.5%. In this work, the average hardness data was calculated basing on the data in depth from 200 to 1000 nm. In the case of WHC05, the hardness of unirradiated specimen is ~ 7.1 GPa, and increases to ~ 7.7 GPa after D irradiation to a fluence of 2.70 × 10^{25} D/m^2, and then to ~ 8.5 GPa after D irradiation to a fluence of 7.02 × 10^{25} D/m^2. That's to say, the hardening rate is less than 9% if the D irradiation fluence is below 2.70 × 10^{25} D/m^2, and reaches up to 19.7% when D irradiation fluence increases to 7.02 × 10^{25} D/m^2. The difference in irradiation hardening with the increasing D irradiation fluence between pure W and WHC05 specimens will investigated systematically through FIB-SEM and TEM analysis, to uncover the factors such as interstitial defects, the type and density of dislocations, which affect the irradiation hardening.

4. Conclusion

In this work, surface blistering and D retention behaviors in pure W and WHC05 exposed to high fluence D plasma irradiation have been investigated. It is found that the irradiated surface areas are covered by vast blisters after D plasma exposure with a fluence above 6.00 × 10^{24} D/m^2 for both the pure W and WHC05. The irradiated area of pure W has large and few blisters, while the WHC05 has smaller but dense blisters. The temperature dependent D desorption peaks appear roughly the same positions for pure W and WHC05 specimens: two main desorption peaks of ~ 560 K and ~ 800 K, corresponding to D release from the intrinsic defects and plasma-induced voids, respectively. While the D retention in pure W is much higher than that of the WHC05. The D irradiation induces an evident hardening in pure W and WHC05. However, due to the effective dispersion of irradiation defects in WHC05, no obvious hardening has been observed in WHC05 beneath the depth of 1500 nm from its surface. After D irradiation to various fluences,

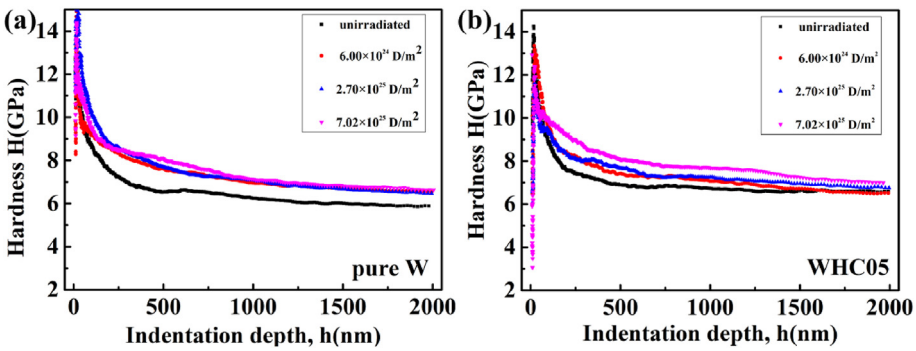

Fig. 5. Indentation depth dependence of nanoindentation hardness of pure W and WHC05.

a hardness value of ~ 7.9 GPa is observed in irradiated pure W specimens, corresponding to a hardening rate of 21.5%. In the case of WHC05, there is a distinct hardening behavior responding to the increase of D fluence: the hardness of unirradiated specimen is ~ 7.1 GPa, while increases to ~ 7.7 GPa after D irradiation to a fluence of 2.70×10^{25} D/m^2, and then to ~ 8.5 GPa after D irradiation to a fluence of 7.02×10^{25} D/m^2, corresponding to hardening rates of 9% and 19.7%, respectively.

Declaration of competing interest

The authors declare that they have no known competing financial interests or personal relationships that could have appeared to influence the work reported in this paper.

Acknowledgments

The authors would like to thank Prof. G.H. Lv and Dr. L. Cheng for their supports with the D plasma exposure experiments in linear plasma device STEP at Beihang University. This work was financially supported by the National Key Research and Development Program of China (Grant No. 2019YFE03110200), the Bengbu University cultivation project (BBXY2019KYQD02, 2021pyxm07), Anhui Province Key R&D Program (202004a05020017), Anhui Provincial Department of Education Programs (KJ2021A1125, KJ2021A1127, KJ2021ZD0141), and the Guangdong Basic and Applied Basic Research Foundation (2020A1515010828).

References

[1] N. Holtkamp, Fusion Engineering and Design 84 (2009) 98–105.
[2] A. Merola, J. Palmer, Fusion Engineering and Design 81 (2006) 105–111.
[3] M. Shimada, R. Pitts, A. Loarte, D.J. Campbell, M. Sugihara, V. Mukhovatov, A. Kukushkin, V. Chuyanov, Journal of Nuclear Materials 390 (2009) 282–285.
[4] P. Norajitra, L.V. Boccaccini, E. Diegele, et al., Journal of Nuclear Materials 329 (2004) 1594–1598.
[5] G.A. Cottrell, Materials science and technology 22 (8) (2006) 869–880.
[6] P. Norajitra, L.V. Boccaccini, A. Gervash, et al., Journal of Nuclear Materials 367 (2007) 1416–1421.
[7] J. Knaster, A. Moeslang, T. Muroga, Nature Physics 12 (2016) 424–434.
[8] D.A. Buchenauer, et al., Gas-driven permeation of deuterium through tungsten and tungsten alloys, Fusion Engineering and Design 109–111 (2016) 104–108.
[9] F. Liu, et al., Gas-driven permeation of deuterium through tungsten with different microstructures, Fusion Engineering and Design 113 (2016) 216–220.
[10] X.X. Zhang, L. Qiao, H. Zhang, et al., Nuclear Materials and Energy 29 (2021), 101079.
[11] H. Kurishita, S. Matsuo, H. Arakawa, et al., Journal of Nuclear Materials 398 (2010) 87–92.
[12] M. Zibrov, et al., Journal of Nuclear Materials 463 (2015) 1045–1048.
[13] X.Y. Li, W. Liu, Y.C. Xu, C.S. Liu, Acta Mater 109 (2016) 115.
[14] Y.K. Wang, Z.M. Xie, et al., International Journal of Refractory Metals and Hard Materials 81 (2019) 42–48.
[15] J.B. Condon, T. Schober, Journal of Nuclear Materials 207 (1993) 1.
[16] A.A. Haasz, M. Poon, J. Davis, Journal of Nuclear Materials 266–269 (1999) 520.
[17] S. Lindig, M. Balden, V.Kh. Alimov, T. Yamanishi, W.M. Shu, J. Roth, Phys. Scr. T138 (2009), 014040.
[18] M. Balden, S. Lindig, A. Manhard, J.-H. You, J. Nucl. Mater. 414 (2011) 69.
[19] G.N. Luo, W.M. Shu, M. Nishi, J. Nucl. Mater. 347 (1-2) (2005) 111–117.
[20] Y. Tan, Y.Y. Lian, F. Feng, et al., Journal of Nuclear Materials 509 (2018) 145–151.
[21] R. Liu, Z.M. Xie, J.F. Yang, et al., Nuclear Materials and Energy 16 (2018) 191–206.
[22] W.M. Shu, M. Nakamichi, V. Kh. Alimov, et al., Journal of Nuclear Materials 390 (2009) 1017–1021.
[23] A. Manhard, U v Toussaint, T. Dürbeck, et al., Physica Scripta T145 (2011), 014038.
[24] B. Tyburska-Püschel, K. Ertl, M. Mayer, et al., Nuclear Fusion 52 (2) (2012), 023008.
[25] Y. Yuan, W. Guo, P. Wang, et al., Nuclear Fusion 59 (1) (2018), 016022.
[26] A.V. Golubeva, M. Mayer, J. Roth, et al., Journal of nuclear materials 363 (2007) 893–897.
[27] Z. Harutyunyan, et al., Vacuum 199 (2022), 110956.
[28] Y. Gasparyan, et al., Journal of nuclear materials 417 (2011) 540–544.
[29] X.X. Zhang, L. Qiao, H. Zhang, et al., Nuclear Fusion 61 (4) (2021), 046026.
[30] X. Liu, R. Wang, A. Ren, et al., Journal of nuclear materials 444 (1-3) (2014) 1–6.